Accelerated in vivo mapping of T_2 relaxation from radially undersampled datasets using compressed sensing and model-based reconstruction

Noam Ben-Eliezer[1], Li Feng[1], Kai Tobias Block[1], Daniel K. Sodickson[1], and Ricardo Otazo[1]
[1]*Department of Radiology, New York University School of Medicine, Bernard and Irene Schwartz Center for Biomedical Imaging, New York, NY, United States*

Introduction Quantitative mapping of transverse relaxation time (T_2) can be used to detect pathological tissue changes in various clinical applications, including identification of edema and iron overload, cancer detection, musculoskeletal imaging, cardiac imaging and more[1-5]. Routine use of traditional (single) spin-echo (**SE**) protocols is impractical due to their long scan times, while faster mapping strategies based on multi-SE (**MSE**) protocols are also inherently biased due to the effects of stimulated or indirect echoes, non-rectangular slice profiles, and B_1^+ field inhomogeneities. Recently, a novel technique for T_2 mapping has been proposed, the echo-modulation curve (**EMC**) algorithm[6], which is able to overcome these penalties of MSE protocols via precise Bloch simulation of the MSE sequence and achieve reliable T_2 quantification in clinically feasible scan times. Radial imaging can be implemented into MSE protocols to provide several benefits including high acquisition efficiency and relatively low sensitivity to physiological motion. Moreover, due to its inherent high incoherence, radial sampling can be accelerated either by using compressed sensing[7-8] (**CS**) or by incorporating an analytical model of the actual acquisition procedure[9-10]. **In this work** we present first results for the fusion of the EMC algorithm with compressed-sensing and model-based reconstruction, aiming to provide accelerated and reliable quantification of both morphological (proton density (**PD**)) and functional (T_2 and B_1^+) information in clinically feasible scan times.

Methods EMC algorithm: Bloch simulations of the prospective MSE protocol were performed using exact RF pulse shapes and other sequence parameters. Simulations were repeated for a range of T_2 and B_1^+ inhomogeneity values (T_2=1…1000ms, B_1^+ = 50…130 %), producing a database of EMCs, each associated with a unique [B_1^+,T_2] value pair. Data were acquired on a whole-body 3T scanner (Siemens TimTrio) for **1)** an $MnCl_2$ phantom and **2)** in vivo human brain using golden-angle radial MSE, and were compared to Cartesian MSE and single-SE protocols with TR=2sec, 3mm slices, {*SE*: TE=15ms, N_{TEs}=6, res=1.7x1.7mm^2, T_{acq}=22min}, {*Radial MSE*: spokes per frame=100, echo-spacing=12ms, ETL=19, res=1.1x1.1mm^2, T_{acq}=3:10min}, {*Cartesian MSE*: echo-spacing=10ms, ETL=22, res=1.1x1.1mm^2, T_{acq}=3:10min (2x GRAPPA acceleration)}. CS reconstruction + EMC fit: Joint multi-coil CS reconstruction[11] was performed for the undersampled radial dataset. A principal-component analysis (PCA) was employed along the echo dimension as a sparsifying transform with empirically selected regularization parameter. This was followed by pixel-by-pixel fitting of the resulting image series to the EMC database via l_2-norm minimization of the difference between experimental and simulated EMCs. PD maps were calculated by extrapolating the first echo image to time t=0 using the fitted T_2 map. Model-based reconstruction: T_2, PD & B_1^+ maps were generated by integrating the EMC database into the signal model of an iterative reconstruction using non-linear conjugate-gradient algorithm[8] implementing a three-parameter [B_1^+,T_2,PD] optimization. Cartesian reconstruction: T_2 maps were generated via EMC fitting of the set of DICOM images produced by the Cartesian MSE.

Results The Figure shows in vivo T_2 and PD maps of the brain of a healthy volunteer obtained using: (**a**) Cartesian single-SE protocol fitted to an exponential decay curve of the form $S(t) = S_0\exp(-t/T_2)$. (**b-c**) Radially undersampled MSE protocol reconstructed using CS and fitted to (b): an exponential model as in 'a', or (c): the database of simulated EMCs. (**e-f**) Radially undersampled MSE reconstructed using an EMC-integrated model-based iterative reconstruction. (**g-h**) Cartesian MSE reference scan reconstructed using the original EMC algorithm. **[**T_2 maps for the **$MnCl_2$ phantom** (not shown) exhibited consistent values for different imaging parameter, pulse-sequence schemes, and MRI scanners.**]**

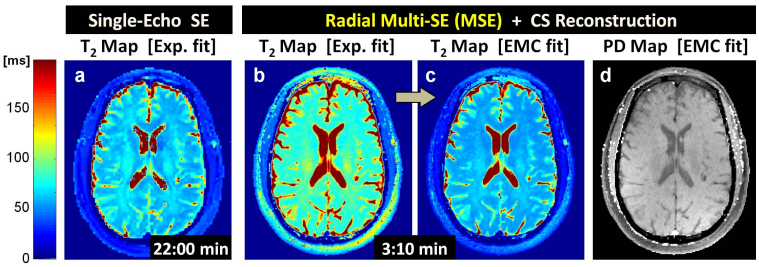

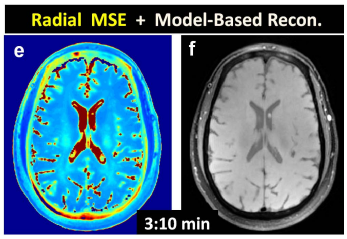

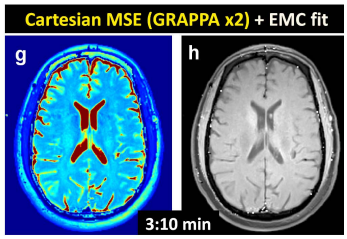

Discussion The EMC algorithm offers fast and accurate extraction of the true sample T_2 values along with other parametric maps such as PD and B_1^+ in a fashion that is scanner and sequence invariant. Its combination with radial sampling offers improved immunity to motion and allows acquisition at arbitrary spatial resolutions owing to the image-folding free nature of radial sampling. Multi-coil CS produced accurate T_2 maps that correlate very well with the reference Cartesian maps, and proved to be more reliable than the model-based approach. This may be attributed to the higher complexity of model-based reconstruction techniques which are usually sensitive to improper parameter scaling and are challenging to optimize[12]. While in theory making less optimal use of the data, the CS-based variant may therefore be the preferable strategy in view of practical applications. The radial EMC framework can be extended to model other contrasts such as T_1, diffusion and T_2^*, multi-compartment T_2 distributions, and various pulse-sequence schemes.

References **[1]** Pan J et al. *Radiology*. 2011; 261(2): 507-15. **[2]** Liu W et al. *MRM*. 2011; 65(5):1400-6. **[3]** Farraher SW et al. *JMRI* 2006; 24(6):1333-41. **[4]** Usman AA et al. *Circ Cardiovasc Imaging*. 2012; 5(6):782-90. **[5]** Patten C et al. *Semin Musculoskelet Radiol*. 2003; 7(4):297-305. **[6]** Ben-Eliezer N et al. *ISMRM* 21, 2013 p 2453. **[7]** Doneva M et al. *MRM* 2010; 64(4): 1114-20. **[8]** Ma D et al. *Nature* 2013; 495(7440): 187-92. **[9]** Block K et al. *IEEE Trans Med Imaging* 2009; 28(11): 1759-69. **[10]** Huang C et al. *MRM* 2012. doi: 10.1002/mrm.24540. **[11]** Feng L et al. *MRM* 2011; 65(6):1661-9. **[12]** Velikina JV et al. MRM 2013; 70(5):1263-73.

Financial support: Helen and Martin Kimmel Award for Innovative Investigation.